Chemical Engineering Journal 160 (2010) 457–465

Contents lists available at ScienceDirect

Chemical Engineering Journal

journal homepage: www.elsevier.com/locate/cej

Analysis and modelling of non-equilibrium sorption of aromatic micro-pollutants on GAC with a multi-compartment dynamic model

Geoffroy Lesage[a,b,c], Mathieu Sperandio[a,b,c], Ligia Tiruta-Barna[a,b,c,*]

[a] Université de Toulouse, INSA, UPS, INP, LISBP, 135 Avenue de Rangueil, F-31077 Toulouse, France
[b] INRA, UMR792, Laboratoire d'Ingénierie des Systèmes Biologiques et des Procédés, F-31400 Toulouse, France
[c] CNRS, UMR5504, F-31400 Toulouse, France

ARTICLE INFO

Article history:
Received 18 September 2009
Received in revised form 18 March 2010
Accepted 19 March 2010

Keywords:
Kinetics
Mass transfer
Diffusion
PAH
Toluene

ABSTRACT

The optimisation of granular activated carbon (GAC) processes for industrial wastewater treatment requires the development of dynamic model that considers adsorption in multi-compartment porous media. In this work, the adsorption of toluene and naphthalene on GAC is investigated. Sorption equilibrium and kinetic experiments were performed at laboratory scale using low contaminant concentrations. The experimental conditions were chosen so as to simultaneously explore the different ranges of concentrations typically encountered in industrial wastewaters. The sorption behaviour was then explained through modelling taking into account the main equilibrium and transport phenomena and three adsorption compartments: the GAC particle surface, the macro- and meso-pores, and the micro-pores. The pore diffusion and solid diffusion were both considered to be coupled with a linear adsorption isotherm. With one set of four parameters adjusted for an adsorbent/contaminant pair, the model satisfactorily describes the non-equilibrium adsorption/desorption processes in different operating conditions and initial conditions.

1. Introduction

Because of industrial and urban development, many hazardous organic substances and micro-pollutants are discharged into the environment via wastewaters [1,2]. Removing chemical contaminants from wastewaters continues to be a central problem in environmental remediation and severe discharge constraints are now imposed by legislation for a number of chemicals [3] like mono-aromatic and polyaromatic hydrocarbons. Adsorption is a well-established technique for the removal of low concentrations of organic pollutants from industrial wastewater. Among the many adsorbents available, activated carbon is effective in removing a large variety of organic components [4]. Treatment options may range from activated carbons that differ in pore structure and surface chemistry to the control of one or more chemical compounds and mixtures. Granular activated carbon (GAC) has been shown to be efficient for the removal of organic micro-pollutants including aromatic hydrocarbons, halogenated hydrocarbons, pesticides, polychlorobiphenyl and surfactants [5]. The optimisation of GAC processes for industrial wastewater treatment demands a good knowledge of the adsorption and desorption dynamics. When GAC is operated in a completely mixed reactor (ref) fed with wastewater, it can be subjected to micro-pollutant concentrations that vary with time, leading to non-equilibrium in the system. Few studies have reported the analysis of this dynamics, which depends on mechanisms of internal diffusion into GAC in different compartments of the granular medium: surface, macro- and micro-porosity.

The present work focuses on two substances typically found in industrial wastewaters: toluene and naphthalene. Toluene and naphthalene have been characterized as potential human carcinogens and their maximum permissible concentrations in drinking water range from 4.6 to 0.3 $\mu g\,L^{-1}$ among different countries [6]. Toluene is a very popular solvent, used in the electronics, chemical and printing industries. Polycyclic aromatic hydrocarbons (PAH) are produced by human activity, chiefly in the pyrolysis and combustion processes employed in industry, transport and heating [7]. These substances cause severe environmental pollution because of their persistence in the environment and their genotoxicity to living organisms. The chemical properties of toluene and naphthalene differ by their volatility and hydrophobicity: toluene is a highly volatile organic compound (VOC) while naphthalene is characterized by lower water solubility and high octanol–water partioning coefficients ($\mathrm{Log}\,K_{ow}$). Naphthalene is one of the most soluble of the PAH and therefore represents the worst case for PAH mobility. In many studies, naphthalene is used as a model chemical for hydrophobic organics. Since GAC is a heterogeneous granular medium with particle sizes ranging from 0.5 to 10 mm, a bimodal pore distribution (macro- and micro-porous) and a high

* Corresponding author at: Université de Toulouse, INSA, UPS, INP, LISBP, 135 Avenue de Rangueil, F-31077 Toulouse, France. Tel.: +33 05 61 55 97 88; fax: +33 05 61 55 97 60.
E-mail address: ligia.barna@insa-toulouse.fr (L. Tiruta-Barna).

1385-8947/$ – see front matter © 2010 Elsevier B.V. All rights reserved.
doi:10.1016/j.cej.2010.03.045

specific surface area (500–2000 $m^2\,g^{-1}$) [8], it is particularly suitable for the efficient sorption of high molecular weight organic molecules with lipophilic properties, as is the case with PAH [9]. Ania et al. [10] found that the adsorption of naphthalene depended strongly on the pore size distribution of the adsorbent, particularly narrow micro-porosity. Although the micro-porous surface constitutes a major fraction of the specific surface area, adsorption of organic micro-pollutants also occurs on the external surface of particles and macro-pore walls. Whereas the experimental characterization of adsorption of GAC is frequent in the literature [10–15], dynamic models that consider adsorption in multi-compartment porous media are rare. The sorption of organic micro-pollutants onto natural and synthetic sorbents has been described as a complex process in which the properties of the sorbate and the solvent play a critical role. The sorption process occurs within the boundary layer around the sorbent and proceeds in the liquid-filled pores or along the walls of the pores of the sorbent. As the classical modelling approaches point out, the adsorption process is composed of several steps:

.

- Diffusion of the pollutant from bulk liquid through the thin film of liquid surrounding the GAC particle (external transfer).
- Pollutant adsorption on the particle's external surface.
- Diffusion inside the pores (internal transfer) by two main mechanisms: pore diffusion (in large pores) and/or surface diffusion (in all pores, particularly in narrow, molecular-size-like pores).
- Adsorption on the pore walls.

Within a perfectly stirred reactor at constant temperature, adsorption rate is controlled by extra- or intra-particular diffusion steps. The relative importance of these steps depends on the adsorbent structure (particle diameter, pore length and diameter), solute properties (solute diffusivities) and hydrodynamic conditions. The design of a full-scale process requires knowledge not only of the equilibrium state but also of the dynamics of the solute adsorption/desorption processes, which depend strongly on the different steps described above.

In most studies, the adsorption rate of organic compounds from aqueous solutions is modelled by using several simplistic mathematical expressions that include the pseudo-first order [16], pseudo-second order [17,18], the intraparticle diffusion model [19,20] and the Elovich model [21]. Although these kinetic equations have been frequently employed to interpret adsorption data obtained under non-equilibrium conditions, their theoretical origins still remain unknown [22]. The specific parameters contained in these equations can be determined only by fitting on experimental data and are dependent on the operating conditions, e.g. the initial sorbate concentrations. Wu et al. [18] observed that, for the same sorbate/sorbent pair, the performance of a given kinetic model depended on the particle sizes. Another common aspect of most studies on PAH adsorption is that the solutions used were relatively concentrated (with respect to the PAH solubility) and prepared using a co-solvent (alcohol), in a narrow range of concentration values.

To describe the equilibrium adsorption, the most commonly used models are the Langmuir and Freundlich models [23,24]. Pikaar et al. [24] have performed a statistical analysis on isotherm models to fit sorption data for the sorption of organic compounds to activated carbon and found that the dual Langmuir equation is, in general, preferable to the single and triple Langmuir equations, the Freundlich equation, a Polanyi–Dubinin–Manes equation, or the Toth equation. Naphthalene adsorption equilibrium in aqueous solution has been studied through the Langmuir–Freundlich single solute isotherm [25,10].

Table 1
Model variables.

Variable	Description	Unit
C	Concentration in the bulk liquid	$g\,m^{-3}$
C^e_{ext}	Equilibrium concentration close to the external surface	$g\,m^{-3}$
C_p	Concentration in the meso- and macro-pores	$g\,m^{-3}$
$\bar{C}_p$	Mean concentration in the meso- and macro-pores	$g\,m^{-3}$
C^e_{mp}	Equilibrium concentration in the liquid phase at the micro-pore inlet	$g\,m^{-3}$
$\bar{C}^e_{mp}$	Equilibrium mean concentration in the liquid phase at the micro-pore inlet	$g\,m^{-3}$
Q	Total quantity adsorbed	$g\,g^{-1}$
Q_{ext}	Quantity adsorbed on the particle external surface	$g\,m^{-2}$
Q_p	Quantity adsorbed in the meso- and macro-pores	$g\,m^{-2}$
$\bar{Q}_p$	Mean quantity adsorbed in the meso- and macro-pores	$g\,m^{-2}$
Q_{mp}	Quantity adsorbed in the micro-pores	$g\,m^{-2}$
$\bar{Q}_{mp}$	Mean content in the micro-pores	$g\,m^{-2}$
r	Radial direction	m
t	Time	s

However, few works have developed physical deterministic models for the explanation of the adsorption kinetics of toluene and naphthalene on activated carbon. Some studies have been conducted on simulation and prediction of pilot plant and full-scale adsorber data, e.g. Crittenden et al. [26], who used a homogeneous solid diffusion model (HDSM) of GAC adsorption of dichloroethylene in a contaminated groundwater matrix. Valderrama et al. [13], have studied PAH removal through GAC adsorption and found that the rate-determining step of PAH extraction is the sorbent-phase diffusion. They used two non-equilibrium adsorption models: the homogeneous particle diffusion model (HPDM) and the shell progressive model (SPM) and have determined PAH effective particle diffusion coefficients (D_{eff}) in the range 1.1×10^{-13} to $6.0 \times 10^{-14}\,m^2\,s^{-1}$. Though many papers dealing with adsorption of organic substances from aqueous solutions have been published [10–15]; the rate and the mechanisms of the adsorption process itself remain unclear. Therefore, it would be appropriate to evaluate a model capable of predicting the equilibrium and kinetic sorption performance of GAC for aqueous trace organic molecules based on fundamental sorbent and sorbate properties.

Therefore, in this paper, aromatics with one and two rings (toluene and naphthalene) are evaluated in a set of sorption and desorption tests on GAC in completely stirred cells, with the following objectives:

- to determine the adsorption behaviour, i.e. kinetic and equilibrium parameters, on an extended time scale (short term to long term), in extreme concentration conditions (low to high) expected to be found in ground and industrial wastewater, i.e. typically in the range of 0.2–200 $g\,m^{-3}$,
- to quantify the main phenomena through a mechanistic modelling approach,
- and to build a model containing a reduced number of adjusted parameters (parameters with a physical meaning) which simulates the adsorption/desorption behaviour in different operating conditions. This model should be easy to handle and resolve and should also allow for its integration in larger models of more complex systems (for example adsorber modelling, or coupling with other bio-physicochemical phenomena).

2. Materials and experimental methods

2.1. Adsorbates and adsorbents

Toluene and naphthalene were supplied by Sigma–Aldrich. Toluene from the BTEX group solvents was chosen as a typical

Table 2
Parameters available from experimental data and measurements.

Parameter	Description	Unit	Experimental value or estimation
a_s	Specific surface area of GAC particles	$m^2\ m^{-3}$	$a_s = f_a(3/R)$; $a_s = 39{,}340$
f_a	Shape factor	–	4.3; estimated by microscope imaging (Fig. 1a)
$C_{0,exp}$	Concentration of the pollutant solution used for adsorption (desorption) experiments	$g\ m^{-3}$	Different experimental values
C_{exp}	Final concentration in an experimental sample	$g\ m^{-3}$	Different experimental values
V	Volume of liquid in the experimental sample	m^3	Different experimental values
R	Particle mean radius	m	3.25×10^{-4} (manufacturer data)
S	GAC mass in the experiments	g	Different experimental values
V_p	Volume of meso- and macro-pores	$m^3\ g^{-1}$	1.1×10^{-7} (BET evaluation)
ρ	GAC particle density	$g\ m^{-3}$	420,000 (manufacturer's data)
ε	Bulk liquid volume fraction		$\varepsilon = \frac{V}{(V+S/\rho)}$
ε_p	Meso- and macro-pore porosity		$\varepsilon_p = \rho V_p$
σ_p	Meso- and macro-pore specific surface area	$m^2\ g^{-1}$	394 (BET evaluation)
σ_{mp}	Micro-pore specific surface area	$m^2\ g^{-1}$	1576.6 (BET evaluation)
σ_{ext}	External surface specific area available for adsorption	$m^2\ g^{-1}$	$\sigma_{ext} = 0.5(a_s/\rho)$

mono-aromatic hydrocarbon, naphthalene was chosen as a model compound for a light molecule of the group of polyaromatic hydrocarbons. All the above chemicals were more than 99% pure. Organic stock solutions were prepared in ultrapure water in a concentration range of approximately 0.2–200 $g\ m^{-3}$.

The granular activated carbon (GAC) employed as the adsorbent was supplied by Pica and had the characteristics presented in Table 2. The GAC was obtained from coconut which was thermally activated and had a mean granulometry of 0.5–0.8 mm. The BET (Brunauer–Emmett–Teller) surface area (1707 $m^2\ g^{-1}$) was obtained from N_2 adsorption isotherms at 77 K on an ASAP2010 micrometrics apparatus. The isotherms were used to calculate the total pore volume, specific surface area and pore size distributions with *t*-plot and HK (Horwath-Kawazoe) modelling. Prior to addition to the vials, the GAC was rinsed three times with ultrapure water to remove dissolved contaminants and fine particles, which could have affected the adsorption capacity of the activated carbon [27,28]. The GAC was then dried at 105 °C for 24 h prior to storage in a dessicator until use [29]. It is generally accepted that activated carbon has a bimodal pore size distribution and contains pores ranging from several microns to a few angstroms. According to the classification by the International Union of Pure and Analytical Chemistry (IUPAC), there are three types of pores: micro-pores having dimensions less than 2 nm, macro-pores larger than 500 nm, and meso-pores lying between these two limits.

2.2. Adsorption of pollutants on GAC

Adsorption measurements of toluene and naphthalene from aqueous solutions on carbon adsorbents were performed at 25 °C in a stirred batch system, which consisted of 120 mL amber glass vials filled without headspace and closed with Teflon-coated septa. Experiments were conducted in laboratory ultrapure water (tap water treated by ion exchange and UV). All points were obtained in duplicate or triplicate. A control sample without GAC was identically prepared for each experiment. The different aqueous solutions of pollutants without solid were first stirred on a rotary stirrer for 72 h. Measurement by GCMS determined the real initial concentration of the solution before the adsorption experiment, taking into account the artefacts associated with the adsorption of pollutants on the different components of the reactor [30]. The GAC was then weighed with an accuracy of ±0.001 g and added into the vials. Tightly closed, the vials were shaken for 2–168 h for the kinetic study. This revealed that the concentration values stabilised (suggesting that equilibrium was reached) in 15 h for NAP and 24 h for toluene (see below). After stirring, the tubes were centrifuged for 20 min at 2500 rpm. The residual pollutant concentration of the supernatant was then determined by GCMS analysis and the adsorbed amount was calculated from the difference between initial and residual concentrations. The adsorbed quantity Q_{exp} is given by the following equation:

$$Q_{exp} = (C_{0,exp} - C_{exp})\frac{V}{S}, \quad (1)$$

where $C_{0,exp}$ and C_{exp} are the initial and equilibrium concentrations respectively ($g\ m^{-3}$), V the volume of solution (m^3) and S is the mass of solid (g).

2.3. Analytical procedures

Pollutant concentrations were determined using a gas chromatograph (Varian 3900), equipped with a mass spectrometer detector (Saturn 2100T) using helium (99.999% purity) as carrier gas coupled with an automatic headspace sampler (Quma HSS40). Separation was accomplished using a 30 m × 0.25 mm × 0.25 μm column (fused silica VARIAN, type VF-5MS (5% phenyl 95% dimethylpolysiloxane)). The water samples (10 mL) were transferred to 20 mL glass vials with Teflon-coated septa and aluminium seals. The samples were equilibrated for 30 min at 80 °C and an aliquot of 1 mL of the headspace gas was injected into the gas chromatograph. The detection limit was 1 $\mu g\ L^{-1}$. The accuracy for measurements of split samples containing a concentration of 1.5 $\mu g\ L^{-1}$ was ±0.1 $\mu g\ L^{-1}$. All vials were first washed and dried in a 500 °C oven to remove all traces of organics.

2.4. SEM analysis

A JEOL 5410LV Scanning Electron Microscope was used to observe the surface morphology of GAC (Fig. 1a). Prior to analysis, samples were dried in a vacuum oven at room temperature and then gold coated.

3. Modelling

The model applied was based on the four-step conceptual model:

- External diffusion of the pollutant through the thin liquid film surrounding the GAC particle.
- Pollutant adsorption on the particle's external surface.
- Internal diffusion by two main mechanisms: pore diffusion (in large pores) and surface diffusion.
- Adsorption on the pore walls.

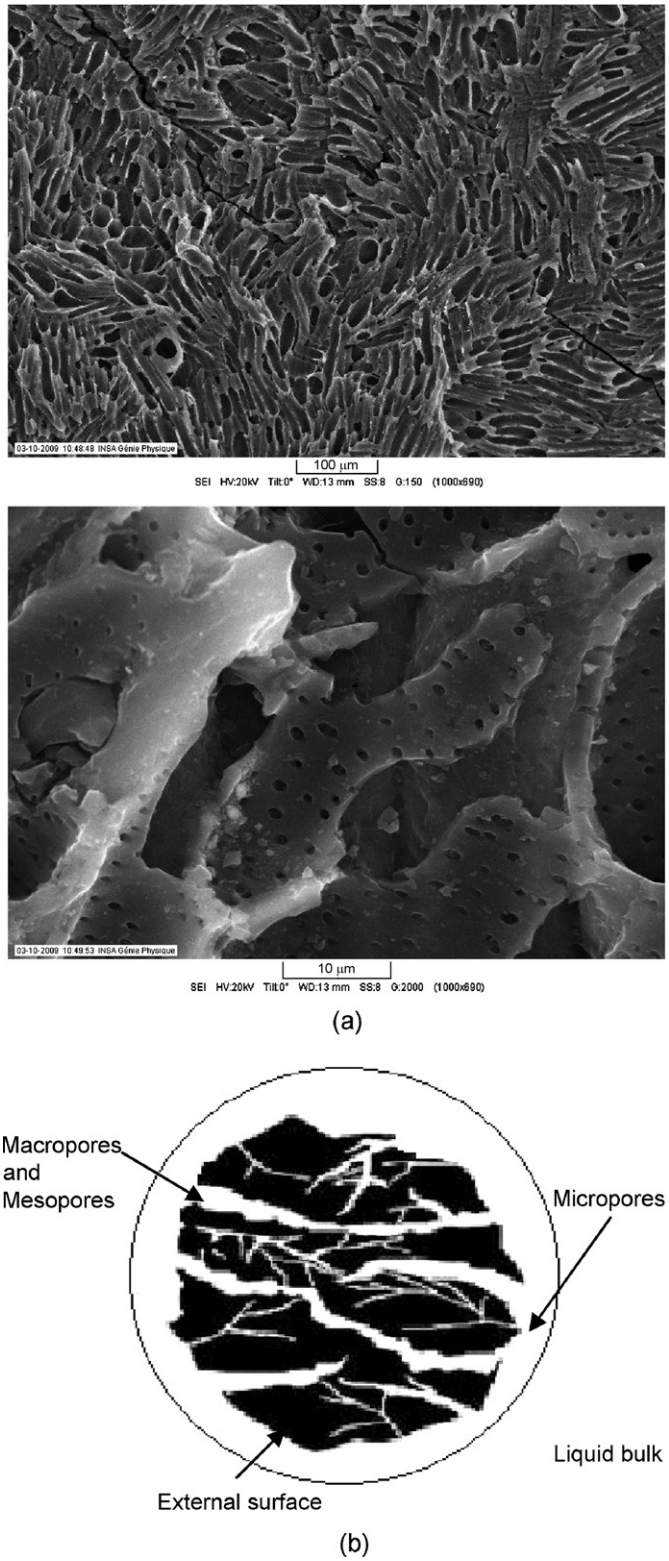

Fig. 1. (a) Scanning electron micrographs of the activated carbon PICAS35; (b) scheme of a GAC particle.

And on the following supplementary assumptions:

- The adsorbent particles are spherical (particle diameter is given by the arithmetic mean value of the mesh size) (Fig. 1b).
- Pores of different sizes are parallel, i.e. transfer between different types of pore is not considered.
- Two main diffusion mechanisms should be taken into account. For large pores (macro- and meso-pores) only the pore diffusion is considered because it is several orders of magnitude faster than the solid diffusion. As the two mechanisms occur in parallel, the slower one can be ignored. For the narrow (micro) pores, only solid diffusion is considered.
- Two pore categories are considered: (1) macro-pores (the ratio of volume to surface area is very small for the macro-pores of the adsorbent studied); (2) micro-pores (pore size < 2 nm).

Consequently, the model contains three adsorption compartments: the external surface, the macro/meso-pores and the micro-pore surfaces (Table 1).

The external transfer is characterized by:

- the specific surface area a_s ($m^2\,m^{-3}$) corresponding to the geometric surface area of the particles of radius R (m),
- the external mass transfer coefficient k_{ext} ($m\,s^{-1}$) associated with this surface.

According to the principles stated above, the dynamic adsorption model was composed of the following equations.

- Macro- and meso-pore diffusion and adsorption (in spherical coordinates):

$$\varepsilon_p \frac{\partial C_p}{\partial t} + \sigma_p \rho \frac{\partial Q_p}{\partial t} = \frac{1}{r^2}\frac{\partial}{\partial r}\left(r^2 D_e \frac{\partial C_p}{\partial r}\right) \tag{2}$$

with the boundary conditions:

$$r = 0, \quad \frac{\partial C_p}{\partial r} = 0 \tag{3}$$

$$r = R, \quad D_e \frac{\partial C_p}{\partial r} = k_{ext}(C - C_{p|R}) \equiv flux_p \tag{4}$$

C is the bulk concentration ($g\,m^{-3}$). For the meso- and macropore compartment: C_p and Q_p are the pore concentration ($g\,m^{-3}$) and adsorbed quantity ($g\,m^{-2}$) at local coordinates of time t (s) and space r (m), D_e is the effective diffusion coefficient ($m^2\,s^{-1}$), ε_p is the porosity, ρ ($g\,m^{-3}$) is the particle density, σ_p is the specific surface area ($m^2\,g^{-1}$), $flux_p$ ($g\,m^{-2}s^{-1}$) is the flux exchanged between the pore compartment and the bulk liquid phase.

- Micro-pores (pore width comparable with the molecular size) solid diffusion:

$$\frac{\partial Q_{mp}}{\partial t} = \frac{1}{r^2}\frac{\partial}{\partial r}\left(r^2 D_s \frac{\partial Q_{mp}}{\partial r}\right) \tag{5}$$

with the boundary conditions:

$$r = 0, \quad \frac{\partial Q_{mp}}{\partial r} = 0 \tag{6}$$

$$r = R, \quad D_s \frac{\partial Q_{mp}}{\partial r} = \frac{k_{ext}}{\sigma_{mp}\rho}(C - C^e_{mp|R}) \tag{7}$$

The flux exchanged between the micro-pores and the bulk liquid is:

$$k_{ext}(C - C^e_{mp|R}) \equiv flux_{mp} \tag{8}$$

For the micro-pore compartment (subscript mp): Q_{mp} is the locally adsorbed quantity ($g\,m^{-2}$), $C^e_{mp|R}$ is the concentration at R in equilibrium with Q_{mp} at R, D_s is the surface diffusion coefficient ($m^2\,s^{-1}$), σ_{mp} is the specific surface area ($m^2\,g^{-1}$), $flux_{mp}$ ($g\,m^{-2}s^{-1}$) is the flux exchanged between the micro-pore compartment and the bulk liquid.

- External transfer and surface adsorption:

$$\frac{dQ_{ext}}{dt} = k_{ext}(C - C^e_{ext})\frac{a_s}{\sigma_{ext}\rho} \quad (9)$$

$$k_{ext}(C - C^e_{ext}) \equiv flux_{ext} \quad (10)$$

Q_{ext} is the quantity adsorbed ($g\,m^{-2}$) on the external surface of particles (variable only in time), C^e_{ext} is the liquid film concentration near the particle side in equilibrium with Q_{ext}, σ_{ext} is the external specific area available for adsorption ($m^2\,g^{-1}$), $flux_{ext}$ ($g\,m^{-2}\,s^{-1}$) is the flux exchanged between the particle external surface and the bulk liquid.

- Bulk liquid mass balance:

The variation of pollutant concentration in the bulk liquid is due to the pollutant fluxes transferred towards the particle's external surface and to the pores.

$$\varepsilon\frac{dC}{dt} = -(a_s flux_{ext} + a_s flux_p + a_s flux_{mp}) \quad (11)$$

The adsorption isotherm is taken to be linear for the concentration range limited by the weak solubility. Saturation was not observed in any set of experiments. The adsorption constant K_e is expressed in $m^3\,m^{-2}$ and represents a partition coefficient between the liquid and the surface. Adsorption is also considered to be rapid and reversible while a physical interaction mechanism is involved; the local equilibrium assumption is adopted in the model. The same linear adsorption equation was applied for all compartments, for example in the macro- and meso-pores:

$$Q_p = K_e C_p \quad (12)$$

$$\frac{dQ_p}{dt} = K_e\frac{dC_p}{dt} \quad (13)$$

The disadvantage of the present model with respect to its resolution and practical applications is the presence of two-dimensional variables C_p, Q_p and Q_{mp} (time and radius). Previous modelling studies of adsorption systems [31,32] revealed the possibility of transforming the models based on partial differential equations (time and space) into simple differential equations (time) in the case of linear absorption, for both pore diffusion and solid diffusion mechanisms.

In this simplified approach, mean concentrations are used instead of the radially varying concentrations. One of the consequences is the possibility of using the "linear driving force" model [33] associated with a global mass transfer coefficient k_0 between the bulk liquid and the pores:

$$\frac{1}{k_{0,p}} = \frac{1}{k_{ext}} + \frac{R}{5D_e} \quad (14)$$

$$\frac{1}{k_{0,mp}} = \frac{1}{k_{ext}} + \frac{R}{5D_s} \quad (15)$$

where $k_{o,p}$ and $k_{o,mp}$ are the overall transfer coefficient for macro- and meso-pores and for micro-pores, respectively ($m\,s^{-1}$).

With these assumptions, the final form of the model becomes:

$$\varepsilon_p\frac{d\bar{C}_p}{dt} + \sigma_p\rho\frac{d\bar{Q}_p}{dt} = a_s k_{o,p}(C - \bar{C}_p) \quad (16)$$

$$\frac{d\bar{Q}_p}{dt} = K_e\frac{d\bar{C}_p}{dt} \quad (17)$$

$$\frac{d\bar{Q}_{mp}}{dt} = \frac{a_s k_{o,mp}}{\sigma_{mp}\rho}(C - \bar{C}^e_{mp}) \quad (18)$$

$$\bar{C}^e_{mp} = \frac{\bar{Q}_{mp}}{K_e} \quad (19)$$

$$\frac{dQ_{ext}}{dt} = \frac{a_s k_{ext}}{\sigma_{ext}\rho}(C - C^e_{ext}) \quad (20)$$

$$C^e_{ext} = \frac{Q_{ext}}{K_e} \quad (21)$$

$$\frac{dC}{dt} = \frac{\varepsilon - 1}{\varepsilon}[a_s k_{o,p}(C - \overline{C_p}) + a_s k_{o,mp}(C - \bar{C}^e_{mp}) + a_s k_{ext}(C - C^e_{ext})] \quad (22)$$

The overscored concentrations $\bar{C}$ and $\bar{Q}$ represent concentrations averaged over the particle with respect to the radial coordinate and hence depend only on the time coordinate. The total adsorbed quantity $Q\,(g\,g^{-1})$ results from a mass balance calculation over the different particle compartments:

$$Q = \sigma_p\bar{Q}_p + \sigma_{mp}\bar{Q}_{mp} + \sigma_{ext}Q_{ext} + \varepsilon_p\frac{S}{\rho}\bar{C}_p \quad (23)$$

The model contains a set of parameters available from experimental data and measurements, listed with their values in Table 2.

The system of equations (Eqs. (16)–(22)) was numerically resolved in MATLAB®. A multi-parameter optimisation procedure was used for fitting the four specific parameters, i.e. K_e, $k_{o,p}$, $k_{o,mp}$ and k_{ext}, based on the objective function OF to be minimized:

$$OF = \frac{1}{n}\sum_1^n\left(\frac{|C_{sim} - C_{exp}|}{C_{exp}}\right)^2 \quad (24)$$

where n is the number of experimental data, and C_{sim} and C_{exp} are the simulated and measured bulk concentrations, respectively.

The model should represent the adsorption process for any initial conditions (adsorption and desorption processes) and contact durations. The complete sets of adsorption experimental data (i.e. kinetics and pseudo-isotherm results) were used for the fitting procedure: about 100 and 70 points for toluene and naphthalene, respectively. Desorption experimental data were then used for model validation.

The model presents the advantages of considering different kinds of pores with their transport specificities and using mean concentrations of a given compartment, thus simplifying the numerical resolution. The principal weakness is that the porous system is considered to be built up only of parallel pores while, in reality, connections also exist between pores. Ding et al. [34] used a model based on two types of interconnected porosity. This model is more realistic but its numerical resolution is not trivial (partial differential equations of second order with complex boundary conditions). Its use for common applications and extensions for adsorber design could be very difficult.

4. Results and discussion

As explained previously, two kinds of experiments were performed: (1) a kinetic study in which the evolution of the eluate concentration was measured versus time; (2) a pseudo-isotherm study in which the evolution of the eluate concentration was measured when the ratio GAC/liquid (i.e. S/L) varied, for a given initial concentration $C_{0,exp}$ and a given constant contact time. Examples of experimental results are given in Fig. 2 for toluene and naphthalene: kinetics obtained for different initial concentration values ($C_{0,exp}$) and isotherms obtained for different $C_{0,exp}$ and contact times.

The experimental results show the dependence of the adsorption kinetics and isotherms on the initial concentration. The explanation of the experimental results is not obvious especially for the atypical behaviour of the isotherms. A tentative application of commonly used isotherm models like those of Langmuir or Freundlich was unsuccessful because the fitted constants were found to be dependent on the concentration domain. The commonly used kinetic models (first or second order) are unable to correctly describe the shape of the kinetic curves on the whole time scale and exhibit a dependence on the concentration domain.

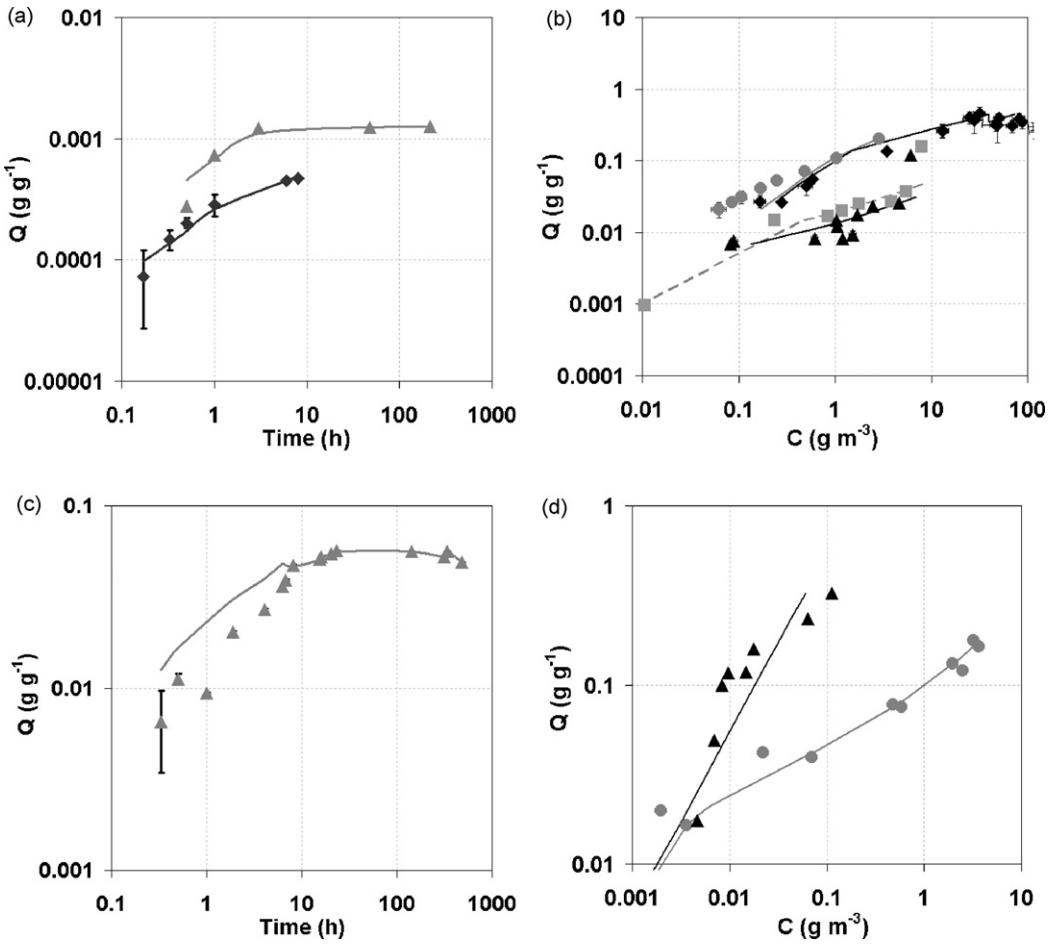

Fig. 2. (a) Adsorption kinetics of toluene at 25 °C, (♦) $C_{0,exp}$ = 5 g m^{-3}; (▲) $C_{0,exp}$ = 13 g m^{-3}. (b) Adsorption pseudo-isotherms of toluene at 25 °C (●) $C_{0,exp}$ = 21 g m^{-3}/contact time = 600 h, (♦) 200 g m^{-3}/94 h, (■) 10 g m^{-3}/48 h, (▲) 7 g m^{-3}/48 h. (c) Adsorption kinetics of naphthalene at 25 °C, (▲) $C_{0,exp}$ = 20 g m^{-3}. (d) Adsorption pseudo-isotherms of naphthalene at 25 °C, (●) $C_{0,exp}$ = 6 g m^{-3}/contact time = 48 h, (▲) 30 g m^{-3}/144 h.

The fact that the isotherms apparently depend on the initial concentration and on the contact time demonstrates that the experimental system was not at equilibrium and this was decisive for the development and application of the conceptual model presented. So, the term "pseudo-isotherm" is more suitable than "isotherm" and will be used hereafter.

The modelling results and the experimental data are represented in Fig. 2 for the kinetic study (Fig. 2a and c) and for the pseudo-isotherms (Fig. 2b and d). The model represents the experimental data in a satisfactory manner.

Table 3 shows the values of the adjusted parameters by molecule. It is important to note that only one set of parameters for each molecule allows the model to correctly predict the overall data obtained in different conditions.

The relevance of the adjusted values of the parameters was assessed through their physical significance.

The constant K_e, having the units of m^3 m^{-2}, is not comparable with other adsorption constant values (in L kg^{-1}) presented in the literature because of the different adsorption models applied and the hypotheses concerning the equilibrium state.

The effective diffusion coefficients (shown in Table 3) for the two types of pores considered in the model were calculated using the formula of Eqs. (14) and (15). The values are reasonable for the type of porosity and diffusion mechanism considered. For reference, the molecular diffusion coefficients in water are 9.5×10^{-10} m^2 s^{-1} and 6.6×10^{-10} m^2 s^{-1} for toluene and naphthalene, respectively.

Finally, the k_{ext} value corresponds to typical values for liquid transfer around solid particles in stirred liquids, which are commonly between 10^{-6} and 10^{-4} m s^{-1}.

The adsorption in a non-homogenous porous matrix is a sequential process in terms of mass transfer and sorbate distribution among the different compartments. If, during the first moments, it is essentially the external surface that is occupied by the sorbate, the prolonged contact time favours a redistribution of the molecules over the different compartments driven by the concentration gradient. This phenomenon depends on the diffusion coefficients and slows down the attainment of an equilibrium state.

The curves in Fig. 3a and b were obtained by simulation using the experimental conditions of the kinetic study in the case of naphthalene (C_0 = 22 g m^{-3}, S/L = 0.04 g L^{-1}) and using the fitted values of the model parameters (as listed in Table 3). For comparison, a simulation was also made with S/L = 4 g L^{-1} and is represented by the grey lines in Fig. 3a.

Fig. 3b shows the total quantity adsorbed Q (Eq. (23)) and the distribution of the sorbent among the different compartments of the GAC particles as calculated by the model: on the external surface ($\sigma_{ext} Q_{ext}$), adsorbed on macro- and meso-pore surfaces ($\sigma_p \bar{Q}_p$), retained in macro- and meso-pore liquid ($V_p \bar{C}_p$), adsorbed in micropores ($\sigma_{mp} \bar{Q}_{mp}$).

Two kinetic domains can be distinguished at different time scales: firstly a short period of several hours corresponding to a massive adsorption on the external surface, followed by a steep

Table 3
Parameters estimated by model fitting procedure and estimated diffusion coefficients.

Parameter	Description	Unit	Toluene	Naphthalene
K_e	Adsorption equilibrium constant	m	2.3×10^{-4}	1.38×10^{-2}
$k_{o,p}$	Meso-pore/macro-pore overall mass transfer coefficient	$m\,s^{-1}$	1.9×10^{-7}	2.2×10^{-6}
$k_{o,mp}$	Micro-pore overall mass transfer coefficient	$m\,s^{-1}$	1.9×10^{-8}	1.9×10^{-8}
k_{ext}	External mass transfer coefficient	$m\,s^{-1}$	1.0×10^{-5}	7.0×10^{-6}
D_e	Effective meso/macro-pore pore diffusion coefficient	$m^2\,s^{-1}$	1.3×10^{-11}	2.1×10^{-10}
D_s	Effective surface diffusion coefficient	$m^2\,s^{-1}$	1.2×10^{-12}	1.2×10^{-12}

decrease in the bulk concentration due to macro-pore adsorption. A pseudo-equilibrium state is observed after about 100 h (for $S/L = 0.04\,g\,L^{-1}$) when the bulk concentration seems to be stabilised but, in fact, a slow increase in the micro-pore adsorption still occurs. A significant evolution of the macroscopic parameters (bulk concentration) would be observed only at very long time periods due to the very slow diffusion in the micro-pores. The influence of solid to liquid ratio on the macroscopic behaviour of the adsorption process is significant, the pseudo-equilibrium state being more rapidly attained for high S/L (grey curves in Fig. 3a). The model used here considers that the different types of pores are independent (parallel), i.e. the micro- and macro-pores do not communicate inside the porous system but communicate directly with the bulk liquid. This is an "optimistic" model because the concentration gradient for micro-porous diffusion is at its maximum (in non-equilibrium adsorption, the bulk liquid is always more concentrated than that in the macro-pores). The simulations show that, even with this optimistic hypothesis, molecules like PAH in aqueous solutions are mostly adsorbed in the macro- and meso-porosity (for short time periods) and thus the use of micro-porous GAC is not necessary.

Among the adjusted parameters, the adsorption constant, K_e, and the mass transfer coefficient for macro- and meso-pores $k_{o,p}$ (or the effective diffusion coefficient D_e) are the most sensitive. Fig. 4a shows a sensitivity study carried out for the kinetic curve of naphthalene. Each curve was calculated by multiplying the parameters K_e, D_e, D_s and k_{ext} by 10, one by one. The sensitivity of a given parameter is not the same over the whole time scale and this result was expected.

The effective diffusion coefficient affects the first period when meso- and macro-pore adsorption takes place. An increase in the adsorption coefficient results in a slowing down of the adsorption kinetics [14] and, obviously, in another equilibrium (pseudo-equilibrium) state. The least sensitive parameter is the solid diffusion coefficient and this is explained by a low adsorption in the micro-pores, at least for the time scale studied. The external mass transfer parameter is not sensitive either; k_{ext} for liquid films in stirred systems takes values between 10^{-4} and $10^{-6}\,m\,s^{-1}$ [35] and, in this range, the simulations are within the experimental data domain. The GAC used in industrial applications has narrow size dispersion so the particle radius should not be a sensitive parameter for a given GAC type. Calculations made with $2R$ and $R/2$ gave

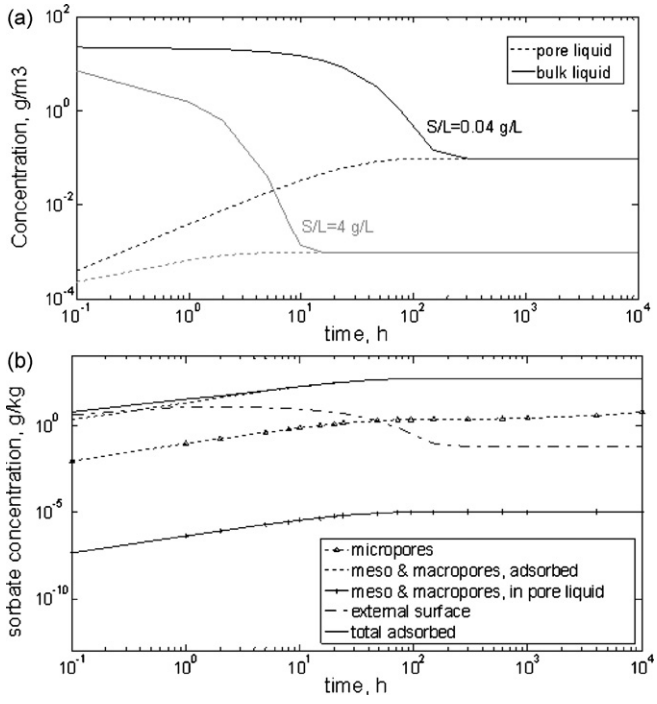

Fig. 3. (a) Simulation of adsorption behaviour: (a) naphthalene concentration ($g\,m^{-3}$) in liquid compartments with two different solid/liquid ratios: $S/L = 0.04\,g\,L^{-1}$ (black lines) and $S/L = 4\,g\,L^{-1}$ (grey lines) with $C_0 = 22\,g\,m^{-3}$. (b) Naphthalene distribution between the particle compartments with $C_0 = 22\,g\,m^{-3}$ and $S/L = 0.04\,g\,L^{-1}$.

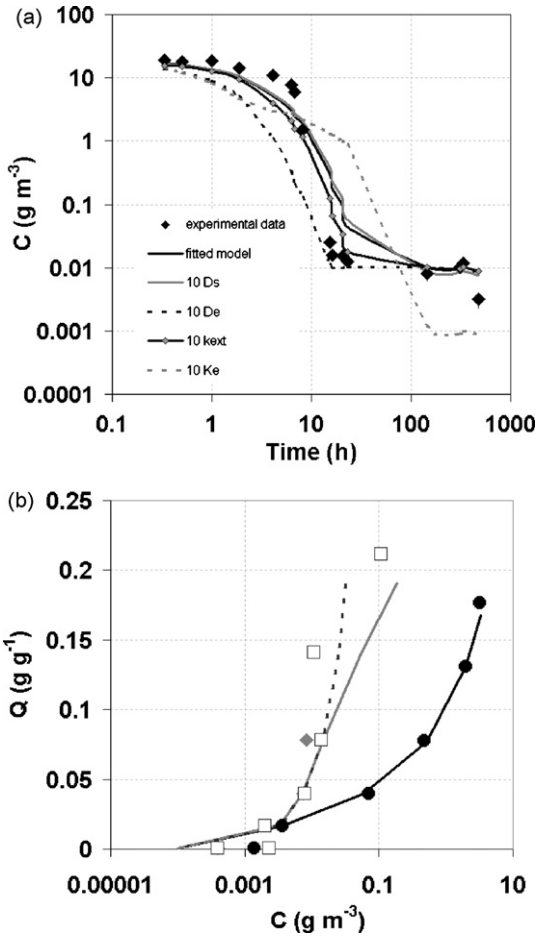

Fig. 4. (a) Sensitivity analysis on adsorption kinetics of naphthalene ($C_{0,exp} = 20\,g\,m^{-3}$). Experimental data (♦) and simulated data (black line), effect of K_e, D_e, D_s and k_{ext}. (b) Pseudo-isotherms of adsorption and desorption of naphthalene at 25 °C, (●) adsorption experimental data $C_{0,exp} = 6\,g\,m^{-3}$/contact time = 48 h; (⧫) first desorption; (□) second desorption; simulated data are represented in line.

the same sensitivity results as k_{ext} (in formula 14 and 15 it is obvious that the diffusion coefficient makes the major contribution to the overall transport).

The model was then confronted with desorption experiments (naphthalene) in order to validate it and to evaluate its predictive performance. The complex experimental protocol composed of an adsorption step followed by two successive desorption steps was simulated using the previously adjusted parameters. As Fig. 4b shows, the simulation results are in agreement with the experimental values.

5. Conclusions

The experimental study of the adsorption/desorption process in various operating conditions and the modelling and simulation work lead to the conclusions drawn below.

(1) The adsorption/desorption of aromatic compounds in aqueous solutions on GAC is a complex process which cannot be represented by simple and usual kinetic models (pseudo-first order, second order, intraparticle diffusion or Elovich) over a wide range of initial concentrations and time periods. These models are not predictive because the equations and parameters contained in them lack physical meaning.
(2) Pseudo-equilibrium states were observed on kinetic curves after about 20 h of contact. Experimental isotherms determined with different initial concentrations and for different contact times clearly show that reaching the equilibrium state requires hundreds of hours.
(3) A multi-compartment dynamic model allowed the deconvolution of the experimentally observed curves and explains the occurrence of many kinetic domains. These kinetic domains are related to the GAC structure and correspond to the different dynamic processes: on the particle surface, in the macro–meso-pores and in the micro-pores. It was expected a priori and then demonstrated by modelling that, at short times, the external surface adsorbs the major part of the solute, then a redistribution of the adsorbed quantity takes place by migration inside the macro–meso-pores and then in the micro-pores, tending towards an equilibrium state in the long term.
(4) Concerning the structure of the model, a set of four parameters characterizing the solute–sorbent interaction (linear adsorption constant and transport parameters) are necessary and cannot be obtained by direct measurements. These parameters are evaluated by fitting the model on a set of experimental data. Once the set of four parameters has been determined, the model becomes predictive for the molecule–GAC pair, being able to simulate the sorption (adsorption–desorption) process in different conditions of concentrations (large range of $C_{0,exp}$), liquid/solid ratios, contact times, initial conditions, etc. This is what was demonstrated by the successful simulation of successive adsorption–desorption experiments in the case of naphthalene.
(5) The modelling and simulation results confirm the experimental observations and show that, for short time periods, the major adsorbed quantity is located on the external surface and in the macro–meso-pores. This conclusion is important for further process design, for the choice of the GAC according to its porous structure and in relation with the process contact time.
(6) The model takes into account the dominant phenomena occurring in the system studied and the specific properties of the adsorbent related to the porous system, being sufficiently complete to describe this kind of system. The principal weakness lies in the parallel pore assumption, the main consequence of which could be a slight overestimate of the micro-porous adsorption (supposition not verified). However, in the case of the system studied (PAH in aqueous solution adsorbed on GAC), the micro-porous adsorption is still very low and hardly useful for a real application. Consequently, the model presented is considered well suited to modelling adsorption/desorption processes for aqueous PAH solutions on GAC.
(7) Besides its predictive character, the model is mathematically simple and easy to solve, and hence it can be easily used in more complex models describing treatment processes and coupled bio-physico-chemical phenomena or it can be used with different adsorption equilibrium laws (non-linear in this case).

Acknowledgements

The authors thank Evrard Mengelle and Gérard Cancel for their technical support. This work was partly supported by the research agency of the French government (ANR). Activated carbon characterization was performed in Ecole des Mines Albi, centre RAPSODEE, campus Jarlard, F-81013 Albi, France.

References

[1] P.T. Williams, Sampling and analysis of polycyclic aromatic-compounds from combustions systems—a review, Journal of the Institute of Energy 63 (1990) 22–30.
[2] P.E.T. Douben, PAHs: An Ecotoxicological Perspective. Ecological and Environmental Toxicology Series, 2003.
[3] Water Framework Directive 2000. Directive 2000/60/EC of the European Parliament and of Council of 23 October 2000 establishing a framework for community action in the field of water policy. Official Journal of the European Communities, pp. 1–72.
[4] A. Seidel, E. Tzscheutschler, K.-H. Radeke, D. Gelbin, Adsorption equilibria of aqueous phenol and indol solutions on activated carbons, Chemical Engineering Science 40 (1985) 215.
[5] J.R. Zimmerman, U. Ghosh, R.N. Millward, T.S. Bridges, R.G. Luthy, Addition of carbon sorbents to reduce PCB and PAH bioavailability in marine sediments: physicochemical tests, Environmental Science & Technology 38 (2004) 5458.
[6] WHO, Guidelines for Drinking Water Quality, World Health Organization Press, Switzerland, 2006.
[7] D. Bouchez, P. Vittorioso, B. Courtial, C. Camilleri, Kanamycin rescue: a simple technique for the recovery of T-DNA flanking sequences, Plant Molecular Biology Reporter 14 (1996) 115–123.
[8] N.P. Cheremisinoff, P.N. Cheremisinoff, Carbon Adsorption for Pollution Control, 1993.
[9] M.T.O. Jonker, A.A. Koelmans, Extraction of polycyclic aromatic hydrocarbons from soot and sediment: solvent evaluation and implications for sorption mechanism, Environmental Science & Technology 36 (2002) 4107–4113.
[10] C.O. Ania, B. Cabal, C. Pevida, A. Arenillas, J.B. Parra, F. Rubiera, J.J. Pis, Effects of activated carbon properties on the adsorption of naphthalene from aqueous solutions, Applied Surface Science 253 (2007) 5741.
[11] M.M. Seredych, V.M. Gun'ko, A. Gierak, Structural and energetic heterogeneities and adsorptive properties of synthetic carbon adsorbents, Applied Surface Science 242 (2005) 154.
[12] C. Valderrama, J.L. Cortina, A. Farran, X. Gamisans, C. Lao, Kinetics of sorption of polyaromatic hydrocarbons onto granular activated carbon and Macronet hyper-cross-linked polymers (MN200), Journal of Colloid and Interface Science 310 (2007) 35–46.
[13] C. Valderrama, J.L. Cortina, A. Farran, X. Gamisans, F.X.D.L. Heras, Kinetic study of acid red "dye" removal by activated carbon and hyper-cross-linked polymeric sorbents Macronet Hypersol MN200 and MN300, Reactive & Functional Polymers 68 (2008) 718–731.
[14] C. Valderrama, X. Gamisans, X. de las Heras, A. Farran, J.L. Cortina, Sorption kinetics of polycyclic aromatic hydrocarbons removal using granular activated carbon: intraparticle diffusion coefficients, Journal of Hazardous Materials 157 (2008) 386–396.
[15] B. Cabal, T. Budinova, C.O. Ania, B. Tsyntsarski, J.B. Parra, B. Petrova, Adsorption of naphthalene from aqueous solution on activated carbons obtained from bean pods, Journal of Hazardous Materials 161 (2009) 1150–1156.
[16] Lagergren, Zur theorie der sogenannten adsorption gelöster stoffe, 24, K. Sven, 1898, pp. 1–39.
[17] V.P. Vinod, T.S. Anirudhan, Adsorption behaviour of basic dyes on the humic acid immobilized pillared clay, Water, Air & Soil Pollution 150 (2003) 193.
[18] F.C. Wu, R.L. Tseng, S.C. Huang, R.S. Juang, Characteristics of pseudo-second-order kinetic model for liquid-phase adsorption: a mini-review, Chemical Engineering Journal (2009).
[19] W.J.J. Weber, J.C. Morris, Kinetics of adsorption on carbon from solution, Journal of the Sanitary Engineering Division 89 (1963) 31–60.
[20] B. Cabal, C.O. Ania, J.B. Parra, J.J. Pis, Kinetics of naphthalene adsorption on an activated carbon: comparison between aqueous and organic media, Chemosphere 76 (2009) 433–438.

[21] S.H. Chien, W.R. Clayton, Application of Elovich equation to the kinetics of phosphate release and sorption in soils, Soil Science Society of America Journal 44 (1980) 265–268.
[22] Y. Liu, L. Shen, From Langmuir kinetics to first- and second-order rate equations for adsorption, Langmuir 24 (2008) 11625.
[23] G. Cornelissen, Gustafsson, Ouml, Predictions of large variations in biota to sediment accumulation factors due to concentration dependent black carbon adsorption of planar hydrophobic organic compounds, Environmental Toxicology and Chemistry 24 (2005) 495–498.
[24] I. Pikaar, A.A. Koelmans, P.C.M. van Noort, Sorption of organic compounds to activated carbons. Evaluation of isotherm models, Chemosphere 65 (2006) 2343–2351.
[25] A. Derylo-Marczewska, M. Jaroniec, D. Gelbin, A. Seidel, Heterogeneity effects in single-solute adsorption from dilute solutions on solids, Chemica Scripta 24 (1984) 239–246.
[26] J.C. Crittenden, D.W. Hand, H. Arora, B.W. Lykins, Design considerations for Gac treatment of organic-chemicals, Journal American Water Works Association 79 (1987) 74–82.
[27] R.S. Summers, P.V. Roberts, Activated carbon adsorption of humic substances. 1. Heterodisperse mixtures and desorption, Journal of Colloid and Interface Science 122 (1988) 367–381.
[28] S.K. Srivastava, R. Tyagi, Competitive adsorption of substituted phenols by activated carbon developed from the fertilizer waste slurry, Water Research 29 (1995) 483.
[29] D.O. Cooney, Z.P. Xi, Activated carbon catalyzes reactions of phenolics during liquid-phase adsorption, Aiche Journal 40 (1994) 361–364.
[30] C.W. Huang, Y.T. Hung, H.H. Lo, Contact oxidation process followed by activated carbon adsorption for textile waste-water treatment, Acta Hydrochimica Et Hydrobiologica 16 (1988) 593–605.
[31] D.D. Do, R.G. Rice, Validity of the parabolic profile assumption in adsorption studies, Aiche Journal 32 (1986) 149–154.
[32] M. Goto, J.M. Smith, B.J. Mccoy, Parabolic profile approximation (linear driving-force model) for chemical-reactions, Chemical Engineering Science 45 (1990) 443–448.
[33] J.I.C.a.E. Gleuckauf, The influence of incomplete equilibrium on the front boundary of chromatograms and the effectiveness of separation, Journal of the Chemical Society (1947) 1315–1321.
[34] L.P. Ding, S.K. Bhatia, F. Liu, Kinetics of adsorption on activated carbon: application of heterogeneous vacancy solution theory, Chemical Engineering Science 57 (2002) 3909–3928.
[35] M. Roustan, Transfert gaz-liquide dans les procédés de traitement des eaux et des effluents gazeux, Lavoisier (2003) 798.